

Asian Journal of **Cell Biology**

ISSN 1814-0068



Ultrastructural Studies on the Effect of Captopril and Furosemide on Some Organs of Albino Swiss Mice

Nabila E. Abdelmeguid, Sherifa S. Hamed and Eglal A. Ahmed Department of Zoology, Faculty of Science, Alexandria University, Alexandria 2151, Egypt

Abstract: The main purpose of the present study was to determine the mechanism by which captopril induces its toxic effect. The study also aimed to determine whether furosemide (a diuretic drug) inhibits or promotes the side effects produced by captopril administration. Two dose levels of captopril were used; low dose (0.01 mg for six days a week, for four weeks) and a high dose (0.23 mg for six days a week, for four weeks). Captopril produced changes in behavioral and external features, changes in the cytological picture of liver and kidney and damage of the cardiac muscle fibers. These changes were found to be statistically proportional to the dose used. Another two groups were studied. One of these groups received the low captopril dose only with furosemide (0.02 mg) and the other received the high captopril dose only with the same furosemide dose for the same period of treatment. Furosemide (0.02 mg) inhibited the decrease in the body weight loss induced by the admission of captopril alone (at both dose levels). It also decreased the mortality rate in mice, but it failed to inhibit the cyto-pathological alterations induced by captopril administration. Despite of the observed damaging effect of the drugs under investigation, they are commonly used as antihypertensive drugs.

Key words: Captopril, furosemide, heart, liver, kidney, ultrastructure

INTRODUCTION

Captopril (D-3-mercapto-2-methyl- propanoyl-L-proline) is an Angiotensin-Converting Enzyme (ACE) inhibitor. Besides, its role as a treatment for hypertension (Sultana *et al.*, 2007), it is commonly used as a cardioprotective drug (Khattab *et al.*, 2005), has the unexpected beneficial side effects such as reducing angiogenesis and tumor growth in rats (Kleinman and Ponce, 1996) and the reduction of both myocardial necrosis and inflammation in mice (Araki *et al.*, 1995).

The histopathological response of the mammalian liver to captopril administration has been tackled by many investigations. Rahmat *et al.* (1985) announced the possibility of hepatic injury and jaundice in patients receiving captopril. Also, Takase *et al.* (1995) observed hepatocytic vacuolar degeneration in dead rats treated with captopril at accumulative dose of 1000 mg kg⁻¹ over a three month toxicity study.

Many investigators studied the effect of captopril administration on kidney of patients and many experimental models. The treatment with captopril caused reduction of glomerular, tubular, vascular and interstitial damage in irradiated, captopril treated rats (Cohen *et al.*, 1996), glomerular sclerosis in rats (Friberg *et al.*, 1994), acute renal failure (Luderer *et al.*, 1981), membranous glomerulopathy and proteinuria (Shearlock and Sturgill, 1983) in patients with hypertension and inhibits the development of functional and morphological damage induced by adriamycin in the kidney of rats (Squadrito *et al.*, 1992).

Furosemide [N-(2-furanylmethyl)-4-chloro-5-sulfamoylanthranilic acid] is a diuretic drug frequently used in the treatment of many cardiovascular and renal diseases (Mitchell *et al.*, 1976). Many reports confirmed that furosemide treatment produces massive hepatic necrosis in mice by a mechanism independent of its diuretic action (Mitchell *et al.*, 1974). It also induced liver damage (Hufnagle *et al.*, 1982), hypertrophy and hyperplasia of the distal convoluted tubule, collecting tubules and cortical collecting ducts in rats (Kobayashi, 1995). Motwani *et al.* (1992) reported that furosemide induced postglomerular vasodilatation in patient with chronic heart failure. Alon *et al.* (1996) studied histological effect of chronic furosemide treatment on kidney of young rats and reported that the most of renal calcification induced by furosemide occur during the early days of treatment in doses of at least 2 mg kg⁻¹ day⁻¹ for at least 12 days.

Furosemide is widely used as an antihypertensive drug, but in patients for whom furosemide treatment alone proves insufficient to reduce hypertension; a common procedure is to co-administer the angiotensin-converting enzyme ACE inhibitor captopril. Mougenot *et al.* (2005) studied the effect of the combination of furosemide and captopril in rats. They suggested that the furosemide/captopril is a rational choice for hypertension treatment and this combination of drugs significantly improved cardiac remodeling and survival of animals.

Owing to the widespread use of captopril in the therapy of hypertension, the present investigation was designed to evaluate its possible adverse effects on major target organs; heart, liver and kidney. The study aims also to determine whether the furosemide (which is a diuretic drug) inhibits or promotes the side effects produced by captopril administration.

MATERIALS AND METHODS

Animals Used

Two hundred adult male mice with average body weight of 25 g and 3-4 month old, were obtained from the animal house of High Institute of Public Health, Alexandria University. Experimental animals were housed in metal cages on wood shaving and had free access to food (carrot, milk and wheat) and drinking water for two weeks prior to the experiment for acclimatization.

Drugs Used

Captopril, (approx. 160 mg mL⁻¹) was purchased from Egyptian International Pharmaceutical Industries. Furosemide was purchased from Hoechst Orient S.A.E. Cairo under License of Hoechst AG Frankfurt (Main), Germany. The dosages were given orally using a clean stomach tube to avoid contamination, between 9 and 11 am. All substances were freshly prepared daily and administrated in volume of approximately 1 mL of sterilized water. The doses of captopril and furosemide used in the present investigation were equivalent to the human therapeutic doses.

Experimental Groups

The experimental animals were divided into five groups, each consist of forty mice.

Group (G1)

Animals of this group received no treatment and considered as control.

Group (G2)

Animals of this group received captopril at a daily dose level equal to 0.01 mg for six days a week, for four successive weeks, i.e., the animal received 0.24 mg/mouse, cumulative dose.

Group (G3)

Animals of this group received captropril at dose level equal 0.23 mg for six days a week, for four successive weeks, i.e., the animals received 5.52 mg/mouse, cumulative dose.

Group (G4)

Animals of this group received captopril at dose level equal 0.01 mg plus furosemide at dose level equal 0.02 mg. Both drugs dissolved in 1 mL of sterilized water, for six days a week, for four successive week, i.e., the animal received; 0.24 mg captopril/mouse plus 0.48 mg furosemide/mouse, cumulative doses.

Group (G5)

Animals of this group received captopril at dose level equal 0.23 mg plus furosemide at dose level equal 0.02 mg. Both drugs dissolved in 1 mL of sterilized water. Animals received both drugs for six days a week, for four successive weeks, i.e., the animal received, 5.52 mg captopril/mouse plus 0.48 mg furosemide/mouse, cumulative doses.

The number of deaths was recorded in each of the five groups as a result of treatment every day while the body weight of each animal was recorded every week and the percentage of mortality was calculated. At the end of experiment and 24 h after the last dose, mice were anaesthetized with chloroform from control and experimental group and organs were fixed (2% glutaraldehyde phosphate buffer) using perfusion technique. After complete perfusion, animals were dissected and small pieces of, myocardium of the left ventricle, liver and renal cortex of kidney were postfixed in 2% glutaraldehyde phosphate buffer for about 2 h at 4°C.

Pieces from the organs were then washed in 0.1 M phosphate buffer, fixed for 1 h in 0.1 M phosphate buffered 1% osmium tetroxide. Dehydration was carried out in ascending series of ethyl alcohol, embedded in epon araldite mixture. An LKB ultramicrotome was used to cut ultra-thin sections, were double stained with uranyl acetate and lead citrate and photographed using Joel 100 CX electron microscope.

Statistical Analysis

Mortality rate, body weight ,measurements of nuclei ,mitochondria and sarcomere are presented as means±SE .One way analysis of variance (ANOVA) was used to assess the significance of changes obtained as a result of drugs treatment. Least significant difference (LSD) at 0.05, 0.01 level of significance was applied to test the significance of difference between the two means.

RESULTS

Determination of Mortality Rate and Body Weight Loss

In the four experimental groups, quantitative results demonstrated a significant increase in mortality rate than control. The highest mortality rate was recorded among animals of G3(Treated with high captopril dose) and reached $32.2\pm3\%$. Animals of the remaining three experimental groups (G2, G4 and G5) showed a lower mortality rate of 25.6 ± 2 , 13.3 ± 3 and $26.7\pm3\%$, respectively. In parallel to the results of the mortality rate, body weight loss in animals of G3 was the highest among all experimental groups and reached $7.6\pm0.3\%$. In the remaining three experimental groups (G2, G4 and G5) the body weight loss showed lower values of 4.4 ± 0.4 , 3.5 ± 0.3 and $4.8\pm0.3\%$, respectively. All the changes in body weight loss were statistically significant (Fig. 1a).

Ultrastructural Observations

Heart

In the control mice, all general aspects of cardiac muscle fiber morphology were evident (Fig. 2a and b). Our morphometeric measurements revealed that the length of control sarcomere is $1.85\pm0.07~\mu m$ (Fig. 1b). The sarcoplasm was distinguished at each pole of the nucleus perinuclear sarcoplasm and filled the spaces between the myofibrils interfibrillar sarcoplasm. Sarcoplasm also,

occupied a thin region between the sarcolemma and the nearest myofibril peripheral sarcoplasm (Fig. 2b). The nuclei were centrally located, ovoid, surrounded by corrugated nuclear envelope with normal chromatin content and having either one or two prominent nucleoli (Fig. 2c). The mean nuclear length of the cardiac muscle of control animals was $13.44\pm1.16~\mu m$ and the nuclear width was $2.27\pm0.2~\mu m$ (Fig. 1b). Mitochondria were distributed in rows between the myofibrils parallel to the long axis of muscle fibers (i.e., interfibrillar mitochondria), or concentrated near the poles of nuclei (Fig. 2b, c) with a length of $0.94\pm0.1\mu m$ and a width of $1.10\pm0.11~\mu m$ (Fig. 1c).

Numerous ribosomes and few small elements of rough endoplasmic reticulum were also present in the sarcoplasm near the nucleus (Fig. 2b). The glycogen particles were found scattered throughout muscle cell sarcoplasm and concentrated between myofibrils (Fig. 2a, b).

In low captopril dose treated group (G2), myofibrils with normal striation were observed, however, a significant decrease in sarcomere length was determined. The nuclei appeared normal,

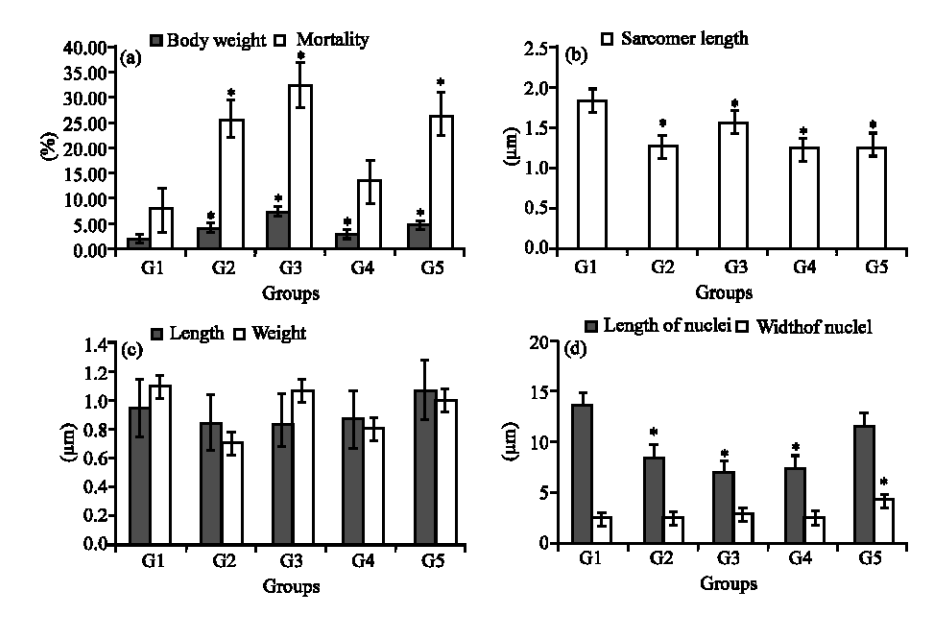


Fig. 1a-d: (a) Mean±SE of percentage values of body weight loss and mortality among various experimental groups. G3 shows the highest mortality and loss of body weight and G4 shows the lowest body weight loss and mortality in comparison to control, (b):Mean±SE of dimensions of myocardial sarcomere length (in μm) among various experimental groups. G3 shows the lowest significant decrease in sarcomere length, while G2 shows the highest significant decrease in sarcomere length in comparison to control, © Mean±SE of dimensions of myocardial mitochondria among various experimental groups. G5 shows the highest value of length and width of mitochondria, while G2 shows the lowest values. Note that all values are insignificant and (d) Mean±SE of dimension of myocardial nuclei among various experimental groups. G5 shows the highest significant value in nuclear width, while G2 shows the highest significant value of nuclear length in comparison to the control. Histogram bars represent mean±SE for percentage of mortality rate, body weight loss, sarcomere length of myocardium and dimensions of nuclei and mitochondria of myocardium, hepatocyte and kidney renal cortex among various experimental groups. Asterisks (*) indicate significant differences compared with controls (p< 0.05, 0.01)

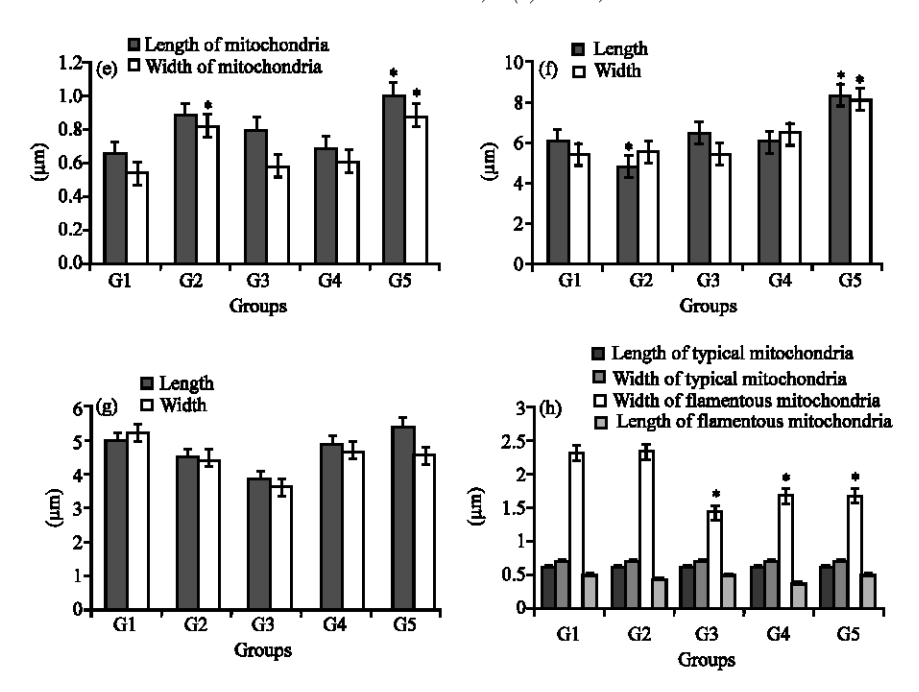
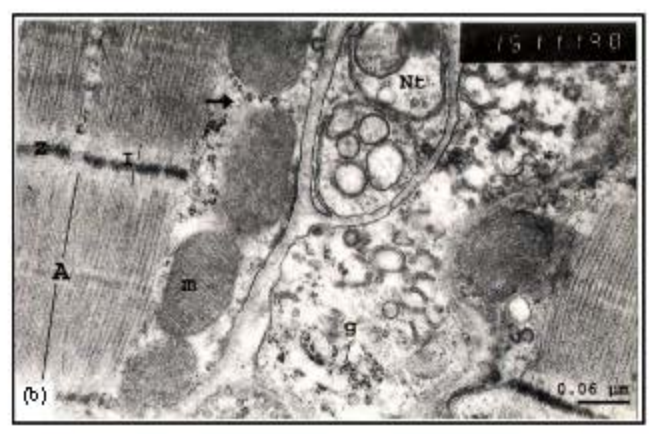


Fig. 1e-h: (e) Mean±SE of dimensions of hepatocyte mitochondria among various experimental groups. G5 shows the highest significant value in all dimensions (length and width) of mitochondria, while G2 shows the lowest significant in comparison to control, (f) Mean±SE of dimensions of hepatocyte nuclei among various experimental groups. G5 shows the highest significant value in all dimensions (length and width), while G2 shows the lowest significant decrease in length in comparison to control, (g) Mean±SE of dimensions of kidney nuclei among various experimental groups. G5 shows the highest value of length, while G4 shows the highest width in comparison to control. Notice that all values are insignificant and (h) Mean±SE of dimensions of typical and filamentous mitochondria of kidney among various experimental groups. In all treated groups, filamentous mitochondria shows a significant decrease in length in comparison to the control except G 2. Histogram bars represent mean±SE for percentage of mortality rate, body weight loss, sarcomere length of myocardium and dimensions of nuclei and mitochondria of myocardium, hepatocyte and kidney renal cortex among various experimental groups. Asterisks (*) indicate significant differences compared with controls (p<0.05, 0.01)

centrally located with more or less normal chromatin content. A significant decrease in length of the nuclei $(8.26\pm1.54~\mu m)$ as compared to the control was observed. However, insignificant decrease in nuclear width and mitochondrial dimensions were also demonstrated (Fig. 1b, c). In addition, an increased number of mitochondria with different shapes and swollen mitochondria with light matrix and disrupted cristae were also observed (Fig. 2d). Hypertrophied Golgi apparatus was observed in the sarcoplasm near the nucleus. Glycogen granules were more frequently observed (Fig. 2d).

After high captopril dose (G3), normal striation appeared side by side to abnormal striation. Significant decrease in sarcomere and nuclear length were observed (Fig. 1b). Most nuclei appeared with abnormal outlines, marginated heterochromatin and abnormal condensed nucleoli. Small, ruptured and vacuolized mitochondria accumulated near the sarcolemma, or scattered among the myofibrils were





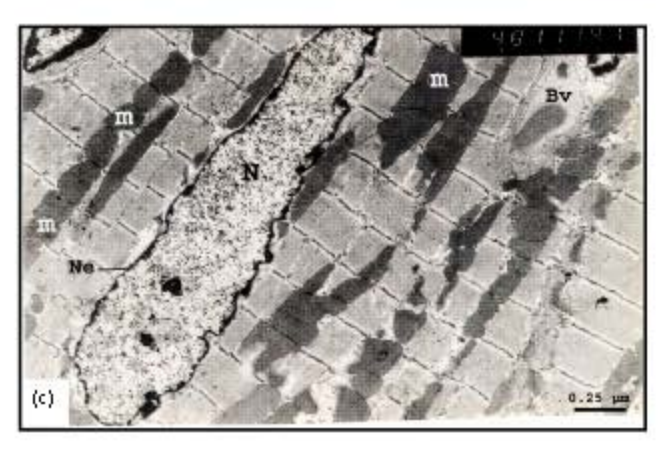
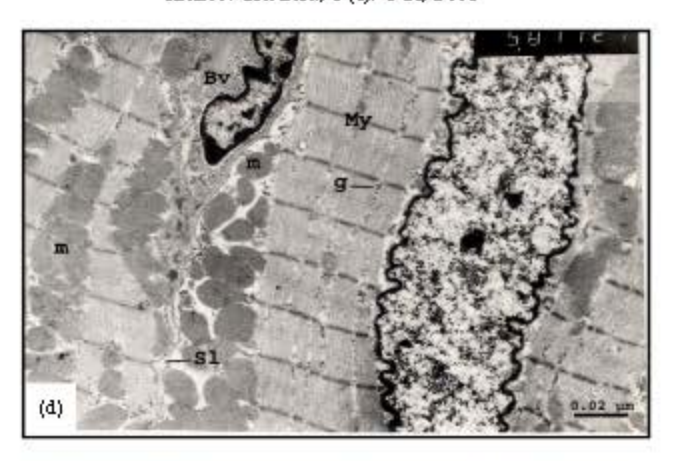
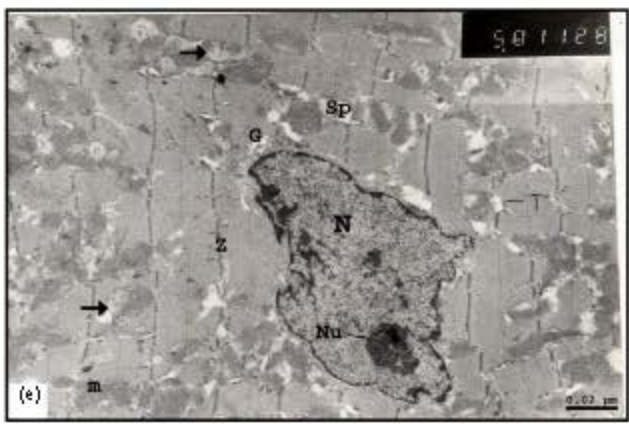


Fig. 2a-c: Election micrographs sections of myocardium of albino Swiss mice. EG1-OsO4 fixed, uranyl acetate-lead citrate stained preparations, (a) Control (GI). Showing alternating bands: dark band (A); Light band (I). Note also that I-b and is bisected by Z-line (Z); the pale area H-b and (H) found in center of A-band and bisected by M-line (M); desosomes (D); glycogen (g), (b) Control (GI). Demonstrating myofibrils, with normal organization A-b and (A), I-b and (I), Z-line (Z). Note the peripheral sarcoplasm (arrow) containing mitochondria (m); glycogen (g); nerve terminal Nt) and (c) Control (GI). Showing normal organized myofibrils; nucleus (N) surrounded with normal nuclear envelope (Ne); mitochondria (m) with uniform dense matrix, blood vessel (Bv)





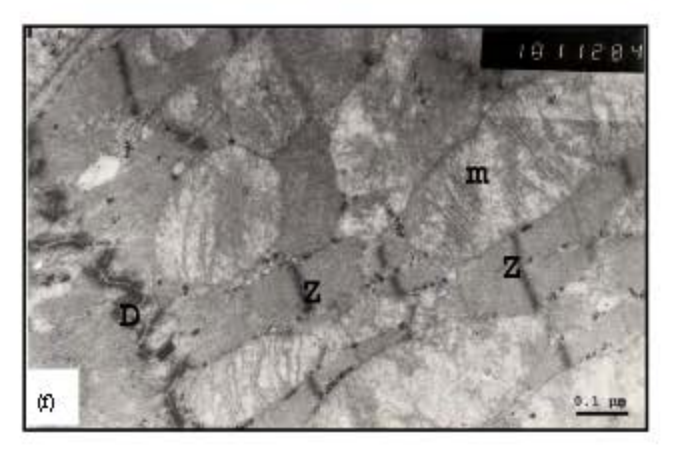
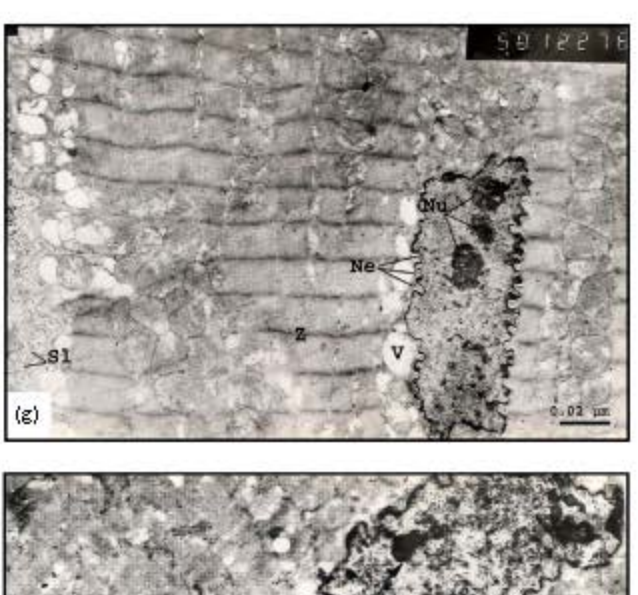


Fig. 2d-f: Electron micrographs sections of myocardium of albino Swiss mice. EG1-OsO4 fixed, uranyl acetate-lead citrate stained preparations, (d) Low dose captopril (G2). Showing myoffb rils (My) with indistinct A and I-bands; Z: Z-line; glycogen(g); sarcolemma (S1); blood vessel (Bv); mitochondria (m) are subsarcolemmal and arranged in between the myoffbrils, (e) High dose captopril (G3). Showing nucleus (N) of cardiac cell with abnormal nuclear envelope; dense nucleolus (Nu); I-b ands are indistinct; distinct Z-line (Z); disorganized mitochondria (m), with damage cristae (arrows); sarcoplasm &p.). Note: Golgi apparatus (G); glycogen(g); T-tubules (T) and (f) High dose captopril (G3). Showing part of cardiac cell that reveal distinct Z-line (Z); megamitochondria (m), with damage cristae; intercalated disk with folding like desomosmes (D)



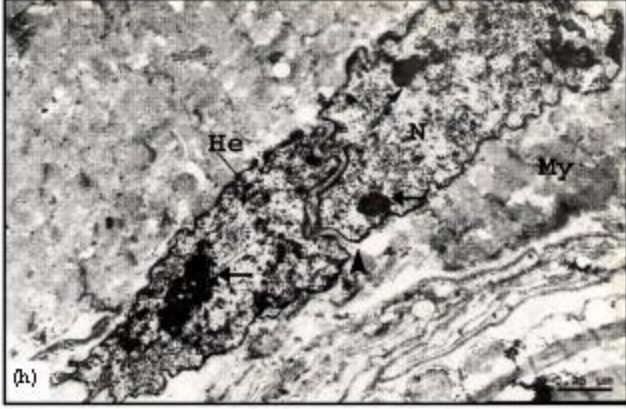


Fig. 2g-h: Electron micrographs sections of myocardium of albino Swiss mice. F₄G₁ – OsO₄ fixed, uranyl acetate-Lead citrate stained preparations, (g) Low captopril dose and furosemide (G4). Altered muscle cells showing nucleus with highly corrugated envelope (Ne) and an increase in the number of nucleoli (Nu). Vacuoles (V), disrupted mitochondria (m), sarcolemma (Sl), Golgi apparatus (G), thick Z-line (Z), (h) High captopril dose and furosemide (G5). Showing severely damage myofibrils (My); nucleus (N) with predominate heterochromatin (He) and number of nucleoli (arrows). Notice also abnormal nuclear division (head arrow)

observed with damage cristae and light matrix (Fig. 2e). Megamitochondria, with irregular arranged cristae and vacuolated matrix were frequently observed (Fig. 2f). The Golgi elements appeared hypertrophied and an increase in glycogen particles was also noticed (Fig. 2e).

Low captopril dose and furosemide treatment (G4) induced alteration of myofibrils cross striations, significant decrease of sarcomere and nuclear length (Fig. 1b, d), nuclear division and increased number of nucleoli (Fig. 2g). Alteration in mitochondrial morphology, distribution, number and dimensions, hypertrophied Golgi vesicles and moderate amount of glycogen were evident. Ruptured and irregular sarcolemma and marked increase in the size and number of lipid droplets in some muscle myocardium were clearly observed (Fig. 2g).

High captopril dose and furosemide treatment (G5) induced significant increase in width of nuclei (Fig. 1d). Most mitochondria were oval or spherical in shape with destructed cristae and vacuolated matrix. A decrease in glycogen particles and ribosome granules and irregular ruptured sacrolemma were also observed (Fig. 2h).

In all studied groups, no significant change in mitochondrial dimensions than control was observed (Fig. 1c).

Liver

In the control mice, all general aspects of liver were observed. It consists of two major cell types, parenchymal cell (hepatocytes) and non-parenchymal cells including Kupffer cells and endothelial cells (Fig. 3a). The hepatocytes appeared with polygonal outline and central round large nuclei with an average of $6.06\pm0.33~\mu m$ length and $6.16\pm0.42~\mu m$ width (Fig. 1f).

The hepatocytes cytoplasm are full with abundant round or ovoid mitochondria, with an average of 0.66±0.05 μm length and 0.54±0.04 μm width (Fig. 1e), Golgi apparatus, rER and sER , lysosome, microbodies and dense aggregates of glycogen rosettes (Fig. 3a).

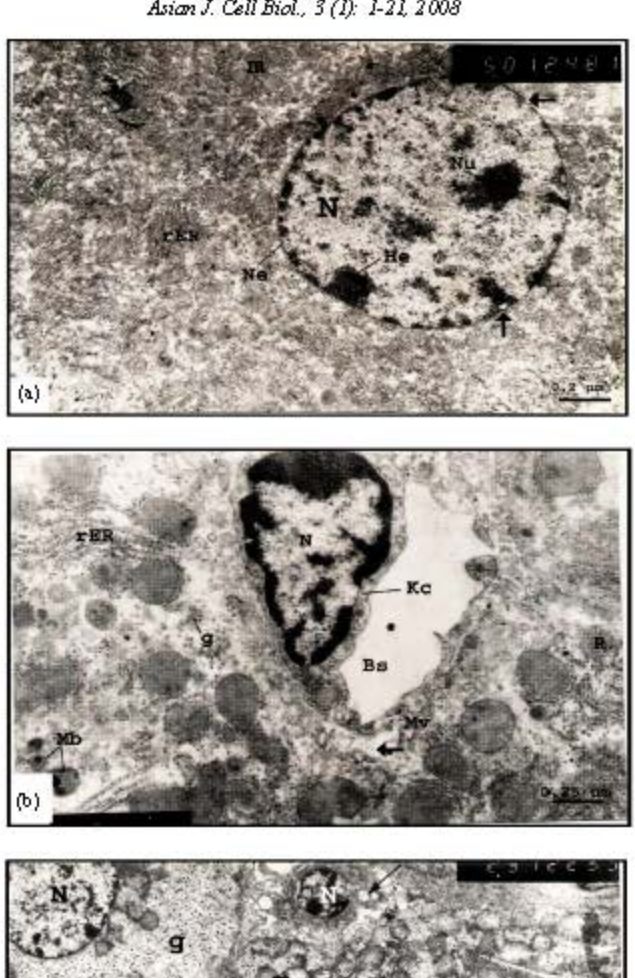
Discontinous fenestrated endothelial cells of blood sinusoids are basal lamina–free and they are separated from hepatocytes by the space of Disse and their wall possess the phagocytic spindle-shaped Kupffer cell with many processes and large oval or triangular nuclei with an average of $4.33~\mu m$ length and $2.00~\mu m$ width (Fig. 3b).

In low dose captopril treated group (G2), hepatocytes showed many altered and pyknotic nuclei, with irregular nuclear envelopes and dilated pores (Fig. 3c). The nuclear dimensions showed significant decrease than control (Fig. 1f). The mitochondria exhibited obvious structural changes, such as disorganization, rupture and disappearance of cristae (Fig. 3c). A significant increase in mitochondrial width was detected in this group (Fig. 1e). In addition, the amount of glycogen granules was similarly increased. Hypertrophied Kupffer cells with vacuolated cytoplasm and large abnormal nuclei were also observed with a mean nuclear length of 4.47 μ m and width of 2.72 μ m, respectively (Fig. 3c).

Liver of high captopril dose treated mice (G3) showed enlarged hepatocytes with cytoplasmic vacuolar degeneration and aggregated dense mitochondria. Mitochondria tended to be oval, elongated, slipper or bizarre shape with fragmented disrupted cristae. Also, the nuclei showed decreased heterochromatin content and an increased number and abnormal segregated, marginated nucleoli (Fig. 3d). In severely affected hepatocytes, rER with loss of ribosomes from their surface were observed. Dilated space of Disse, into which fragmented microvilli projected from the adjacent hepatocyte surface and dilated hepatic sinusoids with hypertrophied necrotic sinusoidal lining cells were observed. There was an increase in the Kupffer cells dimensions than control (an average length of 5.90 μ m and an average width of 2.45 μ m) (Fig. 3e).

In low captopril dose and furosemide treated group (G4), hepatocytes appeared swollen, vacuolated with prominent destroyed nuclei. Few nuclei exhibited marked segregation of their components suggesting their lysis (Fig. 3f), with almost no change in nuclear measurements (Fig. 1f). Mitochondria appeared as either oval or elongated dense clumped bodies, with complete absence of internal structures (Fig. 3f). Complete disappearance or fragmentation of rER, fluctuation in glycogen content and accumulation of moderate lipid droplets were observed. The space of Disse was slightly dilated and the microvilli were fragmented and elongated. Kupffer cells were hypertrophied with an irregular surface. Their nuclei were pyknotic, with predominant heterochromatin (Fig. 3g).

In high captopril dose and furosemide treated group (G5), large, spherical nuclei with slightly irregular nuclear envelope and increased number of nucleoli were seen and the nuclear dimensions increased significantly than control (Fig. 1f). In addition to normal mitochondria, enlarged mitochondria with damaged cristae and dense matrix were also observed (Fig. 3h). The mitochondrial dimension showed a significant increase than controls (Fig. 1e). Degenerated rER, devoid of ribosomes and



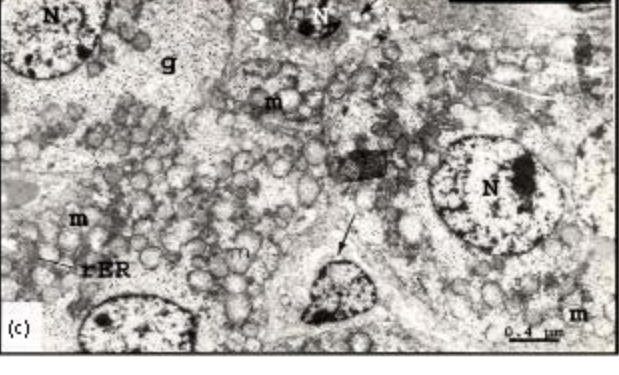
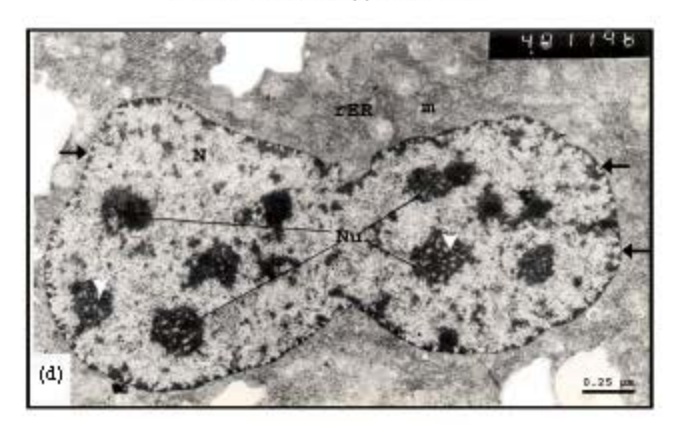
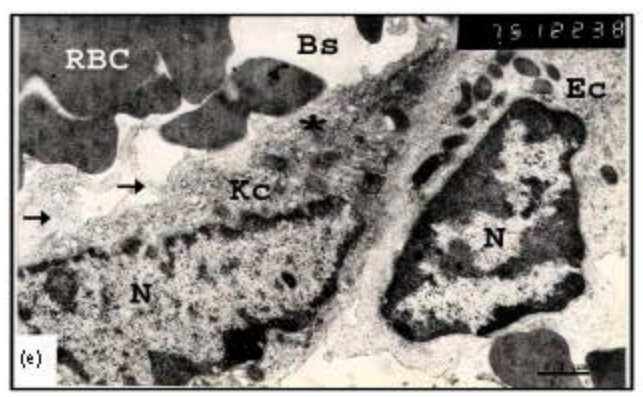


Fig. 3a-c: EM sections of liver of albino Swiss mice. Vascular perfusion with glutaraldhyde; uranyl acetate-lead citrate stained preparations, (a) Control (GI). Showing hypatocyte with large centric nucleus (N) with two compact nucleohis, the heterochromatin (He) occurs in small irregular champs adjacent to nuclear envelope (Ne) and around nucleohis. Note also the nuclear pores (arrows); numerous round or oval-shaped mitochondria (m). Note also the heavily stained rER partially encircling the mitochondria, (b) Control (GI). Showing Kupffer cell (Kc), with triangular nucleus (N); blood sinusoid (Bs). Note sinusoidal surface of hepatocytes with its numerous irregular microvilli (Mv); space of Disse (arrow); microbodies (Mb); glycogen (g); rER; ribosomes (R) and (c) Low dose captopril (GII). Showing a number of hepatocytes with nearly normal nuclei (black N); mitochondria (m), with destructed cristae and enveloped by rER; increased glycogen particles (g); Kupffer cell with vacuolated cytoplasm (anows) and abnormal nuclei (white N)





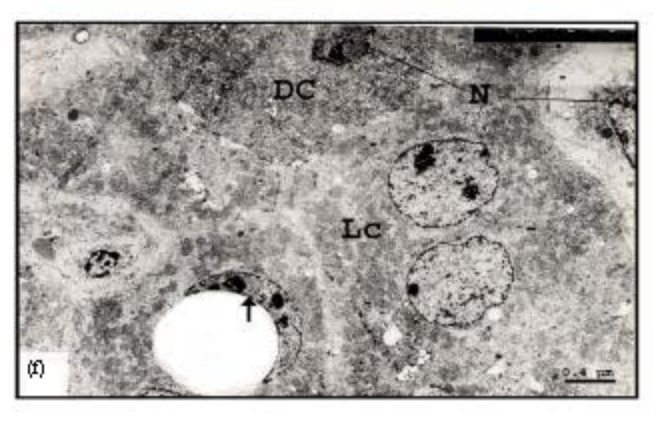


Fig. 3d-f: EM Sections of liver of albino Swiss mice. Vascular perfusion with glutaraldhyde; uranyl acetate-lead citrate stained preparations, (d) High dose captopril (G3). Showing nuclei (N) with abnormal (incomplete) division; increased number of nucleoli (Nu); segregated nucleoli (head arrows); nuclear envelope (Ne) with numerous dilated nuclear pores (anows); mitochondria (m) with damage cristae and vacuolated cytoplasm; fragmented rER; increased ribosomes, (e) High dose captopril (G3). Showing congested blood simisoid (Bs); abnormal blood cells (RBC); hypertophied lining simisoidal cells with hypertrophied nuclei (Kc, Ec). Note also a Kupffer cell (Kc) with its cytoplasmic processes (arrows) and triangular-shaped large nucleus (N); destructed cytoplasm (star) and (f) Low dose captopril and furosemide (G4). Illustrating light (Lc) and dark (Dc) hepatocytes. Note nuclei (N) with abnormal outline and predominate euchromatin, abnormal sinusoidal cell (arrow)

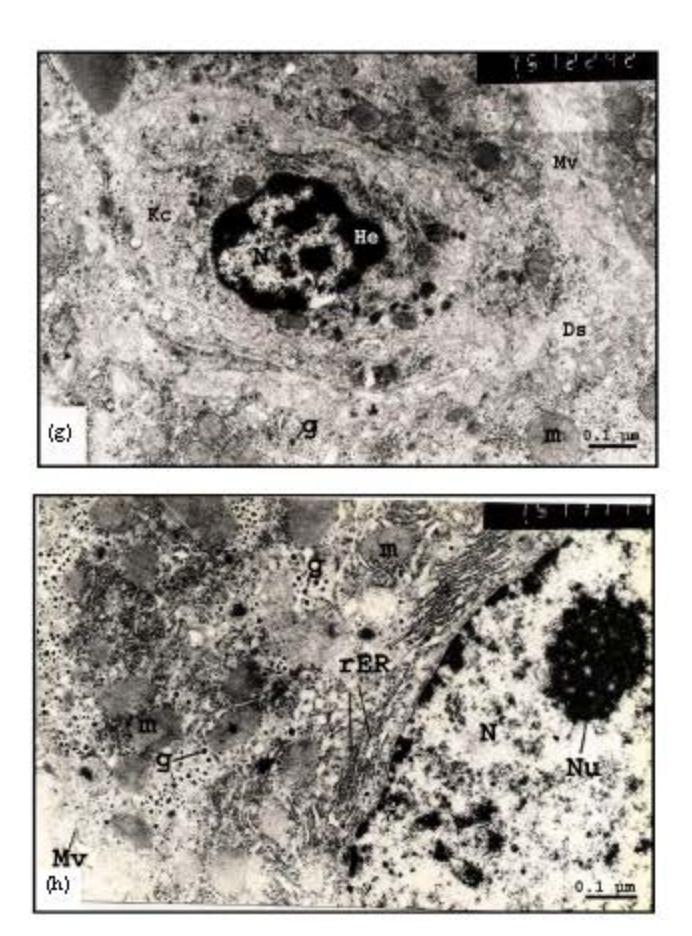


Fig. 3g-h: E.M Sections of liver of albino Swiss mice. Vascular perfusion with glutaraldhyde; uranyl acetate-lead citrate stained preparations, (g) Low dose captopril and furosemide (G4). Showing hypertrophied Kupffer cell (Kc) with altered cytoplasm; nucleus (N) with predominate heterochromatin (He); dilated space of Disse (Ds); damaged microvilli (Mv), glycogen (g), mitochondria (m), (h) High dose captopril and furosemide (G5). Showing part of nucleus (N); segregated nucleolus (Nu); destructed or dilated rER in some region; mitochondria (m) with indistinct details, glycogen (g); microvilli (Mv)

increased glycogen rosettes were pronounced (Fig. 3h). In some hepatocytes, extensive dilation of rER, bile canaliculi, hepatic sinusoids with abnormal sinusoidal lining cells were detected. Most Kupffer cells' nuclei appeared with a bizarre shape and predominant heterochromatin.

Kidney

All the normal features of the mice renal cortex were observed in the control group (Figs. 4a-c). Control kidney cortex revealed that the glomeruli are composed of capillary loops which are lined with a thin layer of flattened endothelial cells that rest on glomerular basement membrane. The capillaries of the glomerulus are supported by mesangial cells which contain a small densely stained nucleus and dense cytoplasm. The visceral layer which is composed of epithelial cells, called podocytes,

has large nuclei and long cytoplasmic extensions called primary processes arised from the cell body. Proximal convoluted tubule cells were cuboidal with large, spherical, centrally or basaly located nuclei and prominent nucleoli. Moreover, basal plasma membrane exhibits numerous infoldings and extends deeply within the cell. The mitochondria are elongate and rod shaped with organized distribution. A poorly developed granular endoplasmic reticulum were observed, the Golgi apparatus appeared well developed, lying near the nucleus (Fig. 4a). Distal convoluted tubule cells appeared cuboidal, with apical spherical nuclei and a few, short apical microvilli. Mitochondria were smaller and basal infoldings were more developed than those of proximal tubule cells (Fig. 4b).

The collecting duct composed of two major types of cells, principal light cells and intercalated cells dark cells. The principal cell is the most numerous cell type and characterized by short microvilli, few mitochondria and centrally located spherical nucleus, complex basolateral membrane with short interdigitating infoldings. The dark cells have many mitochondria located around the nucleus and more elongated microvilli, whereas the basolateral membrane is less intricate than that of the principal cells.

In the present study nuclei of renal tubules appeared with mean length of $4.98\pm0.22~\mu m$ and width of $5.19\pm0.29~\mu m$ (Fig. 1g) and mitochondrial length $0.70\pm0.05~\mu m$ and width was found to be $0.65\pm0.05~\mu m$, while the mitochondrial length of filamentous mitochondria was $2.30\pm0.05~\mu m$ and width was found to be $0.49\pm0.05~\mu m$ (Fig. 1h).

Low captopril dose treated group (G2) showed that only few renal tubules were pathologically altered. The alterations were more obvious in distal convoluted tubules than in the proximal. The nuclei in distal convoluted tubular cells appeared large, with irregular outline. Nuclear envelope of such nuclei appeared with dilated nuclear pores and an increase in the heterochromatin content. The nucleoli were absent. Vacuolated cytoplasm was a prominent feature in both proximal and distal convoluted tubular cells. Mitochondrial structure alterations and thickened basal lamina were more pronounced in case of proximal convoluted tubular cells (Fig. 4d and e). In such cells, pleomorphic disorganized mitochondria were detected, while in distal convoluted tubular cells, some mitochondria appeared normal while others were disrupted.

Animals of high captopril dose (G3), revealed destructed glomerular endothelial cells that appeared with irregular nuclei and destructed cytoplasm. Some processes of visceral cells appeared hypertrophied and mesangial cells with irregular nuclei were observed, in addition to obvious thickened basement membrane (Fig. 4f). Lysosomes of proximal convoluted tubular cells were more frequently increased and showed prominent variation in electron density. The basal infoldings appeared destructed and disorganized. Nuclei of distal convoluted tubule cells showed clumps of marginated heterochromatin (Fig. 4g). Moreover pyknotic nuclei and Pleomorphic and myelinated mitochondria aggregated at the basal side of the cell were frequently observed (Fig. 4g, h). Many cells displayed elongated fragmented and destructed microvilli. Filamentous mitochondria showed a significant decrease in length than normal (Fig. 1h). Collecting duct cells exhibited vacuolated cytoplasm, swollen mitochondria with vesicular cristae and fragmented rER.

The glomeruli of animals of low captopril dose and furosemide treated group (G4) displayed ultrastructural alterations resembling those observed in the previously mentioned treated group (G3). Nuclei of mesangial cell were hypertrophied and fused foot processes were also seen. The epithelial cells of destructed tubules were severely damaged so that their contents were mixed and their lumina appeared to contain cellular debris. Mitochondria of different sizes and shape were disorganized and destructed mitochondria were frequently observed (Fig. 4i)

Examination of electron microscopic preparation of G5 revealed that most of the renal corpuscles and renal tubules were affected. Irregular congested blood capillaries displayed hypertrophied endothelial cells, with large nuclei and destructed vacuolated cytoplasm was observed. Also, mesangial cells revealed irregular shaped nuclei and destructed pale stained cytoplasm. Moreover, the visceral epithelial cells appeared with no definite intact organelles. However, the nuclei were the only intact structure. Also, hypertrophied and fused podocyte processes were commonly observed.

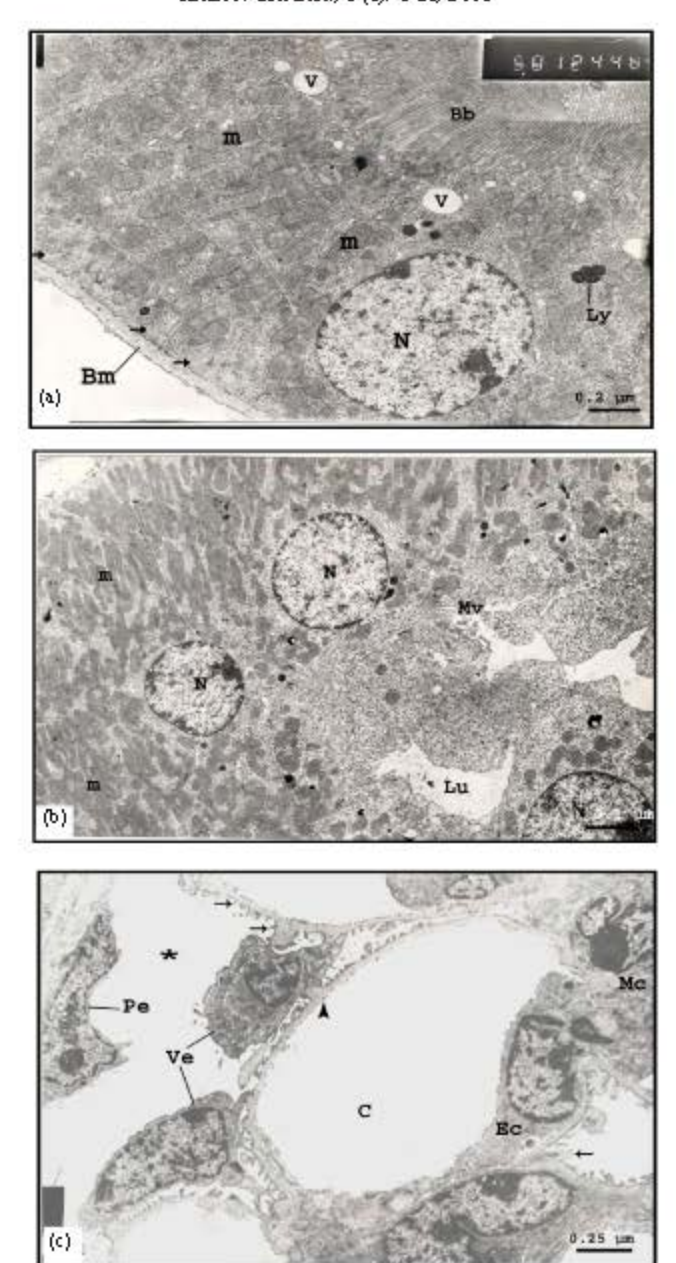


Fig. 4a-c: E.M. Cross sections of renal cortex of albino Swiss mice. vascular perfusion with glutaraldhyd fixed, uranyl acetate-lead citrate stained preparations. (a): Control (GI). Part of proximal tubule with normal large spherical, basally located nucleus (N) and normal chromatin content; numerous well organized mitochondria (m); brush border microvilli (Bb); lysosomes Ly); vacuoles (V). Basement membrane (Bm) exhibits numerous infolding (arrows). (b): Control (GI). Part of distal convoluted tubule, showing apiral spherical nuclei (N), with normal chromatin distribution, mitochondria (m); humen(Lu). Note: short microvilli (Mv). (c): Control (GI). Showing parts of renal corpuscle. Note: parietal epithelium (Pe), urinary space (star), visceral epithelium (Ve) with podocytes (arrow), endothelial cell (Ec), glomenular basement membrane (head arrow), capillary loops (C), mesangial cell (Mc)

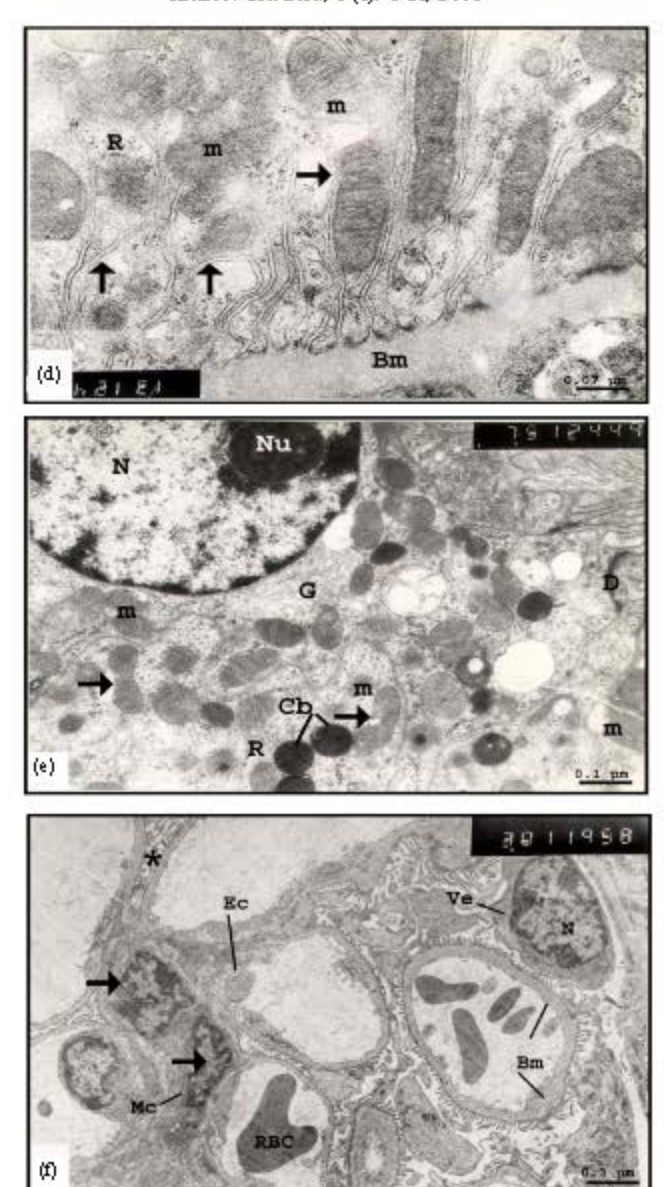
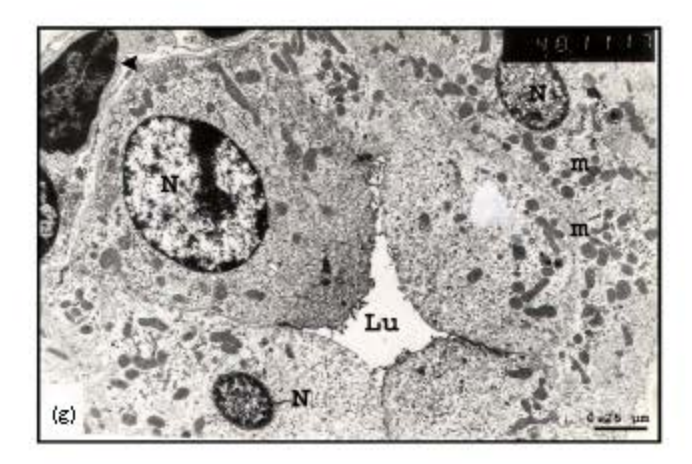


Fig. 4d-f. EM cross sections of renal cortex of albino Swiss mice. vascular perfusion with glutaraldhyd fixed, urarryl acetate-lead citrate stained preparations, (d) Low dose captopril (G2). Basal part of proximal tubular cell with slightly thickened basement membrane (Bm); disorganized, basal membrane infoldings (anows), severely altered mitochondria (m); rbosomes (R), (e) Low dose captopril (GI). Showing apical part of proximal convoluted cell. Note part of nucleus (N), with normal chromatin distribution, obvious nuclelous (Nu); small Golgi vesicles (G); numerous free nbosomes (R) disorganized mitochondria (m), showing many self duplication (arrow), Desomosome (D), cytoplas mic bodies (Cb) and (f) High dose captopril (G3). Showing part of renal corpuscle. Note the capillaries with destructed endothelial cell (Ec); visceral cells (Ve), with large nucleus (N) with a partial fusion of foot processes (star) which form a sheet of epithelial cytoplas m that covers the external surface of the basement membrane (Bm) which is significantly thickened. These features accompany pathological conditions. Note also mes angial cells (Mc) with inegular outline nuclei (anows), compressed red blood cell (Rbc)



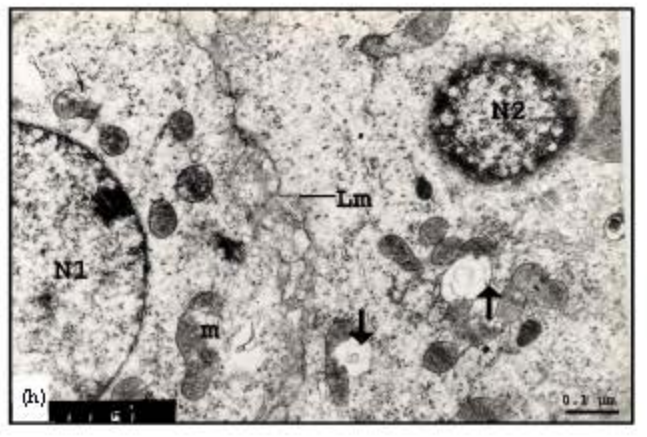


Fig. 4g-h: EM Cross sections of renal cortex of albino Swiss mice. vascular perfusion with glutaraldhyd fixed, manyl acetate-lead citrate stained preparations, (g) High dose captopril (G3). Showing part of distal convoluted tubule cells. Nuclei (N), note marked differences in nuclear size. The peripherally marginated heterochromatin predominates in the nucleus giving a characteristic density of the grazed nucleus, interstitial cell (head arrow), Lumen (Lu); Pleomorphic mitochondria (m) aggregated at basal part. Note the decrease in the number of mitochondria, (h) High dose captopril (G3). Showing two adjacent cells of distal convoluted tubule. Note cell with nearly normal nucleus (N1) and other with pyknotic nucleus (N2); Note slightly irregular lateral membrane (Lm); destructed mitochondria (m) with focal separation of the outer and inner mitochondrial membranes, cavitations of the matrix; vacuoles contain myelin (arrows)

Proximal convoluted tubules were observed with destructed micovilli and infolded basal membrane. Irregular thickened basement membrane was also recognized. Distal convoluted tubules appeared hypertrophied and displayed large elongated nuclei, with irregular nuclear envelope. Epithelial cells of collecting duct appeared swollen with destructed basal infoldings. Mitochondria with indistinct were frequently observed (Fig. 4j). The mean length of filamentous mitochondria decreased significantly than control (Fig. 1h).

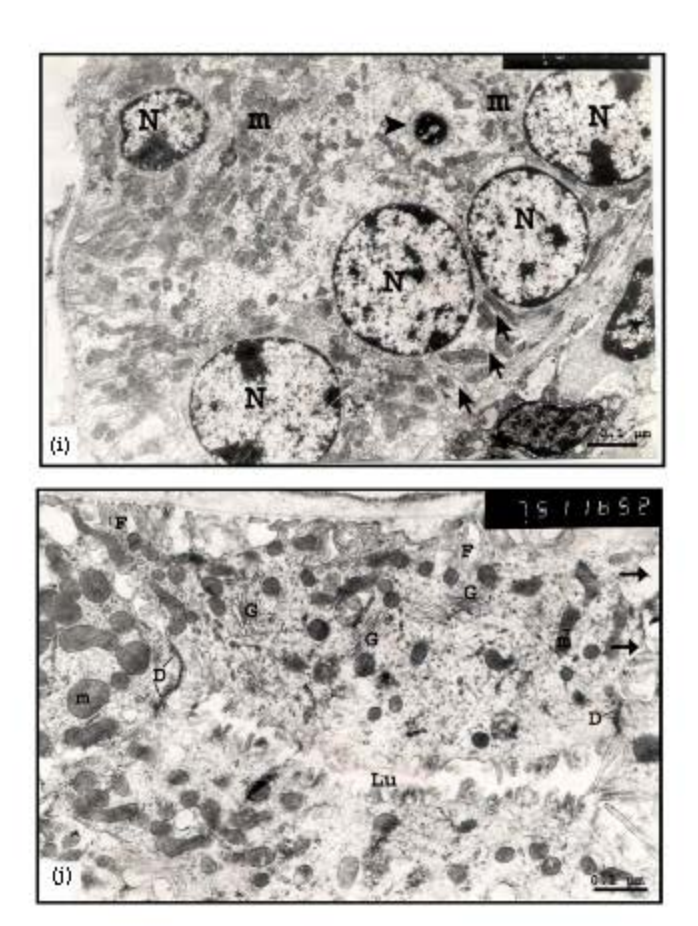


Fig. 4i-j: EMCross sections of renal cortex of albino Swiss mice, vascular perfusion with glutaraldhyd fixed, uranyl acetate-lead citrate stained preparations, (I) Low dose captopril and furosemide (G4). Showing severely damaged part of distal convoluted tubule. Note, less dense, vacuolated cytoplasm; nuclei (N) with abnormal chromatin distribution; necrotic cell with pyknotic nucleus (head arrow); decrease and shortening of basal inflodings (arrows), most of the mitochondria (m) have fragmented, disorganized greatly deformed at the base and apical region. Note also, interstitial cell with margination of chromatin, apparently a step in the development of pyknosis (asterisk), (j) High dose captopril and furosemide (G5). Showing parts of collecting duct cells. Note swollen epithelium with destructed basal membrane infoldings (F); abnormal mitochondria (m), with dense electron dense matrix and indistinct cristae; increased Golgi zones (G); widened intercellular space (arrow); desmosomes (D); narrow lumen (Lu)

DISCUSSION

The present investigation was carried out to examine the mechanism of action that could possibly be correlated with the side effects and the exact cause of damage of three major target organs (heart, liver and kidney), produced as a result of the antihypertensive, captopril, drug administration.

It was found that treatment with captopril resulted in a significant decrease in body weight gain than in normal untreated control, this decrease was dose dependent. Furthermore, it was found that the decrease in body weight in animals treated with captopril alone was greater than the decrease in body weight of animals treated with captopril and furosemide. This could be due to the interaction between furosemide and captopril. Similar observation was described by Squadrito *et al.* (1992), who studied the effect of a daily oral administration of captopril (100 mg kg⁻¹), on the development of functional and morphological alterations induced in rats by single injection (7.5 mg kg⁻¹) of adriamycin. However, Cavanagh *et al.* (1997) studied the effect of captopril on mice reported that treatment with captopril at a dose level of 50 mg L⁻¹ of drinking water for 11 weeks had no effect on their body weight of the mice.

Significant increase in mortality rate among albino Swiss mice was recorded during this experiment after captopril administration (either at low dose or high dose). On the other hand, administration of low captopril dose and furosemide resulted in nearly normal mortality rate as they recorded in the control group. However, furosemide when administrated along with captopril at a high dose decreased the rate of mortality as compared to the group treated with captopril at a high dose alone. However, the mortality rate was still significantly higher than that in the control group. We believe that both captopril and furosemide are drugs that affect mortality. But for some reasons, when both are administrated at the same time and due to their interaction, the mortality rate changed.

These findings were consistent with those of Leor *et al.* (1994) who reported that captopril at dose level 100 mg kg⁻¹, administrated thirty minutes before myocardial damage, failed to improve the survival of rats with acute myocardial infraction. This conception was supported also by Lopez *et al.* (1996) who studied the metabolic effect of the combination of furosemide and captopril in rat and they suggested that the furosemide/captopril combination is a rational choice for hypertension treatment.

Concerning cardiac muscles, morphometric results of the present study showed that the sarcomere length significantly decreased after antihypertensive drug administration as compared to the corresponding control, an evidence that indicates alteration in contractile ability. This finding is in agreement with Hu *et al.* (1990) who demonstrated that administration of captopril at a dose level of 1 mg mL⁻¹ in drinking water for 4-6 weeks reduced or prevented ventrical dilation in rats and Candia Carnevali and Saita (1975) who showed that the length of sarcomere is the most important parameter, of assessing the contractile capacity of any muscle and is a better indicator of the ability of the muscle to maintain protracted tension. Washed striation, disorganized myofibrils, irregular or ruptured sarcolemma were observed in myocardium of all treated animals in the current study. All of these changes may lead to loss of myofibrils, as described previously by Ghadially (1997).

In addition, the results of the present study are in agreement with those of Vulpis *et al.* (1994, 1995), who studied the effect of ACEi on ultrastructure of myocardium of normotensive rats. They observed disarranged myofibrils that were obliquely oriented and smaller than normal, with areas of electron-transparent sarcoplasm separating the myofibril bundles.

During this study, the mitochondria increased dramatically in the myocardium of albino Swiss mice, treated with captopril or captopril with furosemide. The mechanism whereby ACE inhibition leads to increased cellular mitochondria is unknown.

In the present study, giant mitochondrial profiles (megamitochondria) with light configuration were observed in cardiac muscles of animals after administering high captopril dose or high captopril dose with furosemide, a fact that express failure of furosemide to inhibit the alteration induced by captopril administration.

Powers *et al.* (1982) reported that initial captopril administration produced a decrease in coronary blood flow that was related to a decrease in myocardial oxygen requirements. They added that the presence of oxygen was necessary for respiration and glycolysis, which could explain the presence or accumulation of large quantities of glycogen, in the sarcoplasm of animals that received high captopril dose and high captopril dose with furosemide.

The liver is the center of detoxifying and eliminating the toxic substances that are carried to it via the blood. So, it is uniquely exposed to a wide variety of exogenous and endogenous products, which include environmental chemicals and toxins (Wight, 1982).

The present results clearly show that the liver tissues responded markedly to the effect of the antihypertensive drug used. Alterations of nuclei dimensions were observed in hepatocytes of treated animals. Enlargement, margination and irregularity of shape and increased number of nucleoli were observed in hepatocytes of treated animals, an observation similar to that in case of malignancy (Ghadially, 1997).

In this study also, furosemide treated groups showed several alteration in mitochondria of hepatocytes which more or less resemble those produced by low or high captopril dose administration, i.e., furosemide failed to inhibit mitochondrial changes induced by captopril. Present findings are supported by those Klouchek and Popov (1989) who studied the effect of furosemide at a dose level of 300 mg kg⁻¹ on rat liver where they reported that furosemide produced hepatic toxicity. It was also found that the rER in hepatocytes of treated animals appeared damaged or dilated. Some of them appeared completely devoid of the ribosomes. Many studies indicate that the endoplasmic reticulum is a dynamic labile organelle which can readily undergo either hypertrophy or atrophy and there changes usually reflect a state of altered functional activity (Ghadially, 1997).

Many pathological alterations were observed in kidney preparations of treated animals. Distal convoluted tubules in all treated groups were more affected than proximal convoluted tubules. A relationship between the action of drugs used and the function of these tubules could be suggested. This agrees with the finding of Ahmed *et al.* (1992) who studied the effect of naproxen on the kidney of albino rats.

It was also observed that captopril or captopril with furosemide induced many alterations in renal corpuscles. These changes include Bowman's space which appeared nearly normal in animals treated with low captopril dose, obliterated in animals treated with high captopril dose and dilated in animals treated with captopril and furosemide. Similar to our findings, Sakr (1995) observed dilation of the blood capillaries after administration of captopril at a dose level of 60 mg kg $^{-1}$ for one, two and three month in the kidney of mice. Hypertrophied and fused foot processes of podocytes were noticed after using captopril and captopril with furosemide. This is in agreement with Case *et al.* (1980) who noticed that there is an association of proteinuria with captopril treatment in human after administration of captopril in doses ranging from 75 to 600 mg day $^{-1}$ at periods of 4 to 28 months. They also evaluated the possible nephrotoxic side effect of this drug. Therefore, nephrotoxicity of this drug must be weighed against the possible clinical benefit.

It could be concluded that, the marginated chromatin observed in treated animals is a constant precursor of pyknosis in epithelial, endothelial and mesangial nuclei. Even after the nucleus shrinkage the chromatin granules usually remain clumped at the periphery, thus confirming Cook *et al.* (1965) who studied the changes in renal glomeruli during autolysis. Moreover, migration of the nuclei of proximal convoluted tubules cells and distal convoluted tubules cells towards the lumen was a prominent feature in treated specimen and thus is attributed to the effect of the drugs used (captopril and furosemide). This was previously suggested in abnormal circumstances such as osmotic nephrosis (More and Crowson, 1955). Concerning the mitochondria observed in basal part of renal tubular cells, they displayed destructed cristae as well as ruptured membrane. The widening and destruction of basal membrane infolding present in renal tubular cells could be the cause for the disturbance of the basal mitochondrial shape and arrangement. Such renal alterations probably induced acute renal failure as reported by Ponraj and Gopalakrishakone (1997) who studied the renal lesions in rhabdomyolysis caused by *Pesedoechis australis* snake myotoxin.

Moreover, the present results showed a significant decrease in the length of filamentous mitochondria in renal tubules of G3, G4 and G5. This decreases the energy production and thus lowers the efficiency of tubules reabsorption. Micotubules and filamentous mitochondria form together

complex reticula (networks) radiating from the centrosome, which have been observed in cell cultures of neurons and rat kidney cells. Filamentous mitochondrial structures may signify a functional connection between the plasma membrane, the pool of separate mitochondria and mitochondrial clusters (Bereiter-Hahn, 1990; Bereiter-Hahn and Vöth, 1994).

In conclusion, captopril administration at low and high dose induced cyto-pathological alterations in myocardial tissue, liver and kidney at the ultrastructural level in experimental mice. Administration of furosemide inhibited both the decrease in body weight loss and mortality rate induced by the administration of captopril alone, but it failed to inhibit the cyto-pathological alterations.

REFERENCES

- Ahmed, A.M., M.S. Hassan, A.A. ElHawary, K.A. Khalil and A.A. Serwah, 1992. Light and electron microscopic study of the effect of naproxen on the kidney of albino rats pretreated with bovine serum albumin. Egypt. J. Histol., 12: 465-478.
- Alon, U.S., R.A. Kaplan, L.L. Gratny and M.A. Nichols, 1996. Histological long-term outcome of furosemide induced nephrocalcinosis in the young rat. Pediatr. Nephrol., 10: 191-194.
- Araki, M., T. Kanda, S. Imai, T. Suzuki, K. Murata and I. Kobayashi, 1995. Comparative effects of losartan, captopril and enalapril on murine acute mycareditis due to encephalomyocarditis virus. J. Cardiovascular Pharmacol., 26: 61-65.
- Bereiter-Hahn, J., 1990. Behavior of mitochondria in the living cell. Int. Rev. Cytol., 122: 1-63.
- Bereiter-Hahn, J. and M. Vöth, 1994. Dynamics of mitochondria in living cells: Cells shape changes dislocations, fusions and fissions of mitochondria. Microscopy Res. Technol., 27: 198-219.
- Carnevali, M.D.C. and A. Saita, 1975. A typical myofilament arrangement in some abdominal muscles majfly nymphs. Acta Hydrobiol. (Cited in Candia Carnevali and Saita 1976).
- Case, D.B., S.A. Attas, J.A. Mouradian, R.A. Fishman, R.L. Sherman and J.H. Laragh, 1980. Proteinuria during long term captopril therapy. J.A.M.A., 244: 346-349.
- Cavanagh, E.M., C.G. Fraga, L. Ferder and F. Inserra, 1997. Enalapril and captopril enhance antioxidant defenses in mouse tissue. Am. J. Physiol., 272: R 514-R518.
- Cohen, E. P., A. Molteni, P. Hill, B.L. Fish, W.F. Ward, J.E. Moulder and F.A. Carone, 1996. Captopril preserves function and ultrastructure in experimental radiation nephropathy. Lab. Invest., 75: 349-360.
- Cook, M.L., L. Osvaldo, J.D. Jackson and H. Latta, 1965. Changes in renal glomeruli during autolysis. Electron microscopic observations. Lab Invest., 14: 623.
- Friberg, P., B. Sundelin, S.O. Bohman, A. Bobik, H. Nilsson, A. Wickman, H. Gustafsson, J. Petersen and M.A. Adams, 1994. Renin angiotensin system response to ACE inhibition or angiotensin 2 antagonism. Kidney Int., 45: 485-492.
- Ghadially, F.N., 1997. Ultrastructural Pathology of the Cell and Matrix. 4th Edn., Butter. London.
- Hu, Z., M. Billingham, M. Tuck and B.B. Hoffman, 1990. Captopril improves hypertension and cardiomyopathy in rats with pheochromocytoma. Hypertension, 15: 210-215.
- Hufnagle, K., S.N. Khan, D. Penn, A. Cacciarelli and P. Williams, 1982. Renal calcification a complication of long term furosemide therapy in pretem infants. Pediatric, 70: 360-363.
- Khattab, M.M., A. Mostafa and O. Al-Shabanah, 2005. Effects of on Cardiac Captopril on Cardiac and Renal Damage and Metabolic Alterations in the Nitric Oxide-deficient Hypertensive Rat. Kidney Blood Press Res., 28: 243-250.
- Kleinman, H.K. and M.L. Ponce, 1996. Captopril blocks vessel and tumor growth. J. Clin. Invest., 98: 599.
- Klouchek, E. and A. Popov, 1989. Experimental liver damage by furosemide studying drugs with heptoprotective activity. Eksp. Med. Morfol., 28: 47-50.
- Kobayashi, I., 1995. Comparative effects of losartan, captopril and enalapril on murine acute myocarditis due to encephalomyocarditis virus. J. Cardiovascular Pharmacol., 26: 5-61.

- Leor, J., N. Bloom, D. Hasdai, Z. Ovadia and A. Battler, 1994. Failure of captopril to attenuate myocardial damage neutrophil accumulation and mortality following coronary artey occlusion and reperfusion in rat. Angiology, 45: 717-724.
- Lopez, R., C. Toboada, C. Rivas and S. Miguel, 1996. Metabolic effect of combination of furosemide and captopril in rat. J. Physiol. Biochem., 52: 89-94.
- Luderer, J.R., A.C. Schoolwerth, R.A. Sinicrope, J.O. Ballard, D.P. Lookinbill and A.H. Hayes, 1981.
 Acute renal failure hemolytic anemia and skin rash associated with captorpil therapy. Am. J. Med., 71: 493-496.
- Mitchell, J.R., W.Z. Potter, J.R. Hinson and D.J. Jollow, 1974. Massive hepatic necrosis caused by furosemide. Nature (Lonedon), 251: 508-511.
- Mitchell, J.R., W.L. Nelson, W.Z. Potter, H.A. Sasame and D.J. Jollow, 1976. Metabolic activation of furosemide to a chemically reactive, hepatotoxic metabolite. J. Pharmacol. Exp. Ther., 199: 41-52.
- More, R.H. and C.N. Crowson, 1955. Glomerulotubular nephrosis correlate with hepatic lesions 1. A morphologic investigation of the changes of progressive autolysis in human, rabbit and rat tissue. A.M.A. Arch. Path., 60: 63.
- Motwani, J.G., M.K. Fenwick, J.J. Morton and A.D. Struthers, 1992. Furosemide induced natriuresis is augmented by ultra low dose captopril but not by standard doses of captopril in chronic heart failure. Circute, 86: 439-445.
- Mougenot, N., R. Bos, A. Mediani and P. Lechat, 2005. Captopril-furosemide survival study in experimental heart failure. Fundam. Clin. Pharmacol., 19: 457-464.
- Ponraj, D. and P. Gopalakrishnakone, 1997. Renal lesions in rhabdomyolysis caused by *Pseudoechis australis* snake myotoxin. Kidney Int., 51: 1956-1969.
- Powers, E.R., K.S. Bannerman, J. Stone, D.S. Reison, E.L. Escala, A. Kalischer, M.B. Weiss, R.R. Sciacca and P.J. Cannon, 1982. The effect of captopril on renal coronary and systemic hemodynamics in patients with severe congestive namics heart failure. Am. Heart J., 104: 1203-1210.
- Rahmat, J., R.L. Gelfand, M.G. Gelfand, J.F. Winchester, G.E. Schreiner, H.J. Zimmerman and D.C. Washington, 1985. Captopril associated cholestatic jaundice. Ann. Intern. Med., 102: 50-56.
- Sakr, A.A., 1995. Renal and hepatic lesions induced by captopril. Egypt J. Histol., 18: 209-219.
- Shearlock, K.T. and B.C. Sturgill, 1983. Membranous glomerulopath and nephrotic syndrome after captorpil therapy. J.A.M.A., 250: 2343-2345.
- Squadrito, F., G. Macchiarelli, G. Stantoro, V. Arcoraci, G.R. Trimarchi, R. Struniolo, S.A. Nottola, P.M. Motta and A.P. Caputi, 1992. Effect of captorpil on the development of rat doxorubicin nephropathy. Histol. Histopathol., 7: 223-229.
- Sultana, N., M.S. Arayne and R. Quraish, 2007. In vitro interactions of captopril with h(2)-receptor antagonists. Pak. J. Pharm. Sci., 20: 132-139.
- Takase, K., T. Ikuse, H. Aono and A. Okahara, 1995. Toxicity study of the angiotensin converting enzyme inhibitor rentiapril in rats. Arzneim. Forsch., 45: 15-18.
- Vulpis, V., L. Rocali, M. Bertossi, B. Nico, T. Seccia, S. Ricci and A. Pirrelli, 1994. Left ventricular hypertrophy in the spontaneously hypertensive rat effect of ACE inhibitors on ultrastructural morphology. Cardiol., 84: 14-24.
- Vulpis, V., T.M. Seccia, B. Nico, S. Ricci, L. Roncali and A. Pirrelli 1995. Left ventricular hypertophy in the spontaneously hypertensive rat: Effect of ACE inhibitors on myocardiocyte ultrastructure. Pharmacol. Res., 32: 375-381.
- Wight, D.G.D., 1982. Atlas of Liver Pathology. Lancaster, MTP Press Ltd.